Chord-distribution functions of three-dimensional random media: Approximate first-passage times of Gaussian processes

A. P. Roberts*

Princeton Materials Institute and Department of Civil Engineering and Operations Research, Princeton University, Princeton, New Jersey 08544

S. Torquato[†]

School of Mathematics, Institute for Advanced Study, Princeton, New Jersey 08540

The main result of this paper is a semianalytic approximation for the chord-distribution functions of three-dimensional models of microstructure derived from Gaussian random fields. In the simplest case the chord functions are equivalent to a standard first-passage time problem, i.e., the probability density governing the time taken by a Gaussian random process to first exceed a threshold. We obtain an approximation based on the assumption that successive chords are independent. The result is a generalization of the independent interval approximation recently used to determine the exponent of persistence time decay in coarsening. The approximation is easily extended to more general models based on the intersection and union sets of models generated from the isosurfaces of random fields. The chord-distribution functions play an important role in the characterization of random composite and porous materials. Our results are compared with experimental data obtained from a three-dimensional image of a porous Fontainebleau sandstone and a two-dimensional image of a tungsten-silver composite alloy. [S1063-651X(99)06005-5]

PACS number(s): 02.50.−r, 05.40.−a, 81.05.Rm, 47.55.Mh

I. INTRODUCTION

The statistical characterization and modeling of two-phase disordered microstructure is a central problem in many fundamental and applied sciences [1]. Predicting the properties of disordered materials relies on the availability of accurate microstructural models, which rely in turn on accurate statistical characterization. After the volume fraction of each phase, and interfacial surface area, the most important statistical quantity is the two-point correlation function which is obtained from cross-sectional micrographs, or small-angle scattering experiments. Although the two-point correlation function is very useful, there are a variety of important problems where more detailed statistical information is necessary. Another useful characteristic of microstructure, which has proved essential in theory and application, is the chord-length distribution function [2]. The chord functions play an important role in stereology [3], mineralogy [4], the interpretation of small-angle x-ray scattering data [5], and have been incorporated in theories of mass transport in porous media [6]. Recently the chord functions (and the related ''lineal-path'' function [7]) have been employed in the generation of three-dimensional (3D) microstructural models for predicting macroscopic properties [8–10]. In this paper, we derive approximate forms of the chord functions for a relatively new model of random media based on Gaussian random fields.

*Permanent address: Center for Microscopy and Microanalysis, University of Queensland, Brisbane, Queensland 4072, Australia.

[†]On sabbatical leave. Permanent address: Princeton Materials Institute and Department of Civil Engineering and Operations Research, Princeton University, Princeton, NJ 08544.

A useful model of two-phase random porous and composite media is obtained by modeling the internal interface of the microstructure as the isosurface (or level cut) of a correlated Gaussian random field $y(\mathbf{r})$ [11–15]. A region of space can be divided into two phases (e.g., pore and solid) according to whether $y(\mathbf{r})$ is less or greater than some threshold. We define phase 1 to occupy the region where $y(\mathbf{r}) \leq \beta$ and phase 2 to occupy the region where $y(\mathbf{r}) > \beta$. This is illustrated for two dimensions in Figs. 1(a) and 1(b). The model, and variants, have proved useful in describing the microstructure of many different materials [8,16,17]; and a more thorough characterization of the microstructure is an important goal. The two- and three-point correlation functions of the model can be calculated, but the chord functions are presently measured from simulations [8,17]. There are advantages (for speed, accuracy, and interpretation) in obtaining analytic expressions for the chord functions of the model. As we show, the problem is equivalent to finding the probability density governing the time it takes for a Gaussian random process to first cross an arbitrary threshold. This is a conventional first-passage time problem.

First-passage time problems arise in many branches of physics [18], information theory [19], queuing theory [20], ocean science [21], and reliability studies in the engineering sciences [22] among others. For this reason the problem has received a great deal of attention. Rice actually provided a formal series solution to the problem for Gaussian processes [23]. However, the series involves very difficult integrals of which only the first is generally evaluated [18]; the results being accurate for small time. There are many approaches to finding useful approximations for first-passage times (the aforementioned references provide reviews of the literature in each field). Here we restrict attention to methods based on the assumption that the lengths of successive chords are in-
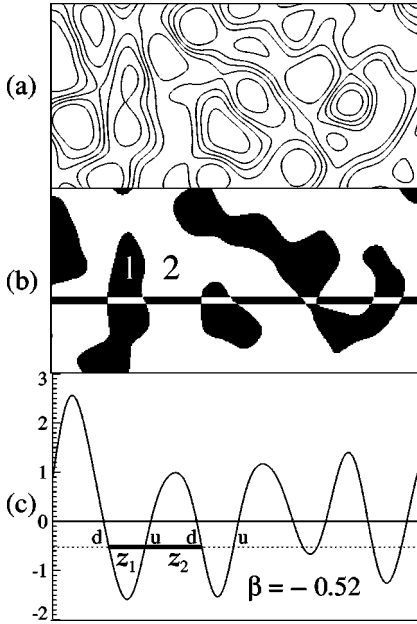
FIG. 1. Generation of a two-phase model (b) by thresholding a Gaussian random field (a). The chord length distribution functions are calculated by counting the number of chords of a given length (b). In one dimension the chord lengths z_1 and z_2 are defined by up and down crossings (shown as u and d, respectively) of a threshold β by a random process (c).

dependent. This idea can be traced back to Siegert [24] and McFadden [25]. The approximation we use is most clearly derived from the independent interval process [5,26] for which the assumption of independent chords is true by definition. This approach was recently suggested for the calculation of persistence times in coarsening [27,28]. The method can be extended to obtain the chord distributions, and actually provides an extremely useful way of viewing related problems in different fields. In the following sections we derive some properties of the chord function and the independent interval process. The model is then applied to approximate the chord functions of level-cut Gaussian random fields. Finally, we compare the theoretical results with experimental data.

II. CHORD-DISTRIBUTION FUNCTIONS

For a two-phase medium, there is a chord distribution associated with each phase $p_i(z)$ ($i=1,2$). The quantity $p_i(z)dz$ is defined as the probability that a randomly chosen chord in phase i (a line segment with end points on the phase interface) has length in the range $[z,z+dz]$. In Fig. 1(b), we illustrate calculation of $p_1(z)$ and $p_2(z)$ for isotropic media: An ''infinite'' line (or many shorter ones with arbitrary orientation) is drawn through the material, and the number of chords in phase 1 [$N_1(z)$] with length in the range $[z,z+dz]$ is counted. If N is the total number of chords of phase 1, then $p_1(z)dz=N_1(z)/N$. The quantity p_2 is defined in an analogous manner. An important quantity is the number of phase crossings per unit length $n_c=2N/L$. A fundamental relation in stereology gives $n_c=\frac{1}{2}s_v$ where s_v is the specific surface, i.e., the surface area to total volume ratio of a 3D composite. Another useful relation follows from the fact that

total length of the chords is equal to that of the original line: $\Sigma_z N_1(z)z+\Sigma_z N_2(z)z=L$. If we divide by N and convert the sums to integrals we have $\int p_1(z)zdz+\int p_1(z)zdz=2/n_c$. Similarly $\Sigma_z N_i(z)z=\phi_i L$ where ϕ_i is the volume fraction of phase i. This gives the relation $\langle z_i \rangle=\int p_i(z)zdz=2\phi_i/n_c$. These equalities are used extensively below. A useful statistical quantity is the lineal-path function of each phase $L_i(z)$ ($i=1,2$), which represents the probability that a random line segment of length z thrown into the material falls completely within phase i and is related to $p_i(z)$ by $L_i(z)=\frac{1}{2}n_c\int_z^\infty p_i(x)(x-z)dx$ [7].

One reason for the usefulness of the chord function is that $p_i(z)$ can be directly interpreted in terms of observable microstructure features. First, if $p_i(0)\neq 0$ then, at the resolution at which it is measured, phase i contains sharp corners. Second, the value at which $p_i(z)$ takes a maximum value provides an estimate of the length scale associated with phase i. Another is provided by the average chord length $\langle z_i \rangle$. Third, if $p_i(z)\neq 0$ for large z, connected regions in phase i at scale z exist. This ''connectedness'' information (along a lineal path) is clearly important if long-range phenomena (like macroscopic properties) are to be studied. The direct relationship between $p_i(z)$ and morphology shows that the chord functions give a strong ''signature'' of microstructure and are therefore an important tool in the characterization of porous and composite media.

The chord and lineal-path functions are closely related to first-passage times in the theory of stationary time-dependent random processes. The analogy is shown in Fig. 1(c). If the values of a random field along a line are plotted against time a one-dimensional random process $y(t)$ is obtained. If a down crossing of the threshold β occurs at $t=t_d$ [so $y(t_d)=\beta$], the probability that the process first exceeds the threshold in the interval $[t_d+t,t_d+t+dt]$ is $p_1(t)dt$. The corresponding density for the first down crossing after an up crossing (sometimes called the second-passage time) is $p_2(t)$. There are several other common first-passage times which relate to our work. Suppose $y(t)$ is a random process representing the response of an electrical or mechanical component which fails if $y(t)$ exceeds some (generally high) threshold [$y(t)>\beta$]. A key quantity is the probability of failure $F(t)$ in the interval $[0,t]$ [29]. Since the safe region is phase 1 the failure probability is just $F(t)=1-L_1(t)$ [$F(0)=1-L_1(0)=\phi_2$ being the probability of instantaneous failure]. A related quantity is the probability distribution of failure times $f_1(t)$ given that $t=0$ is in the safe region [22]. This is given by $f_1(t)=-L_1'(t)/\phi_1$.

III. INDEPENDENT INTERVAL PROCESS

The independent interval process [5,26] is constructed by taking the lengths of successive intervals to be independent of one another and distributed according to the probability (chord) distribution functions $p_1(z)$ and $p_2(z)$ for phase 1 and 2, respectively (this implies a stationary process). Since this completely defines the process it is possible to derive all other statistical properties (such as the two-point correlation function) from $p_1(z)$ and $p_2(z)$. The indicator function $I(\mathbf{x})$ (which is unity in phase 1 and zero in phase 2) is very useful in this regard. From above we have

$$n_c = \langle |I'(\mathbf{x})| \rangle = \frac{2}{\langle z_1 \rangle + \langle z_2 \rangle}, \qquad (1)$$

$$\phi_1 = \langle I(\mathbf{x}) \rangle = \frac{1}{2} n_c \langle z_1 \rangle, \qquad (2)$$

$$\phi_2 = \langle 1 - I(\mathbf{x}) \rangle = \frac{1}{2} n_c \langle z_2 \rangle. \qquad (3)$$

Note that the results are true irrespective of correlations between successive chords.

Now consider the two-point correlation function which is defined as

$$S_{11}(x) = \langle I(\mathbf{x}_1) I(\mathbf{x}_2) \rangle. \qquad (4)$$

Stationarity of the process (and isotropy in more than one dimension) implies that the average only depends on $x = |\mathbf{x}_2 - \mathbf{x}_1|$. To express S_{11} as a function of p_1 and p_2 it is necessary to derive some preliminary results. The method is adapted from Ref. [27]. Although the model is independent of any random field it is useful to describe the left-hand ends of chords in phase 1 and 2 as down crossings and up crossings, respectively (see Fig. 1). Consider the probability $R_{u1}(x)$ that a point at distance x to the right of an up crossing (or right-hand end of a chord in phase 1) falls in phase 1. Suppose the chord (of phase 2) immediately to the right of the down crossing has length z_2. If $z_2 > x$ then the point falls in phase 2. If $z_2 < x$ the chance that the point falls in phase 1 is $R_{d1}(x - z_2)$, where $R_{d1}(y)$ is the probability that a point at distance y to the right of a down crossing falls in phase 1. Thus

$$R_{u1}(x) = \int_0^x dz_2 p_2(z_2) R_{d1}(x - z_2). \qquad (5)$$

Now consider the converse problem for $R_{d1}(x)$. Let z_1 be the length of the first chord (of phase 1) to the right of a down crossing. The probability that a point a distance x from the down crossing falls in phase 1 is unity if $z_1 > x$ and $R_{u1}(x - z_1)$ if $z_1 < x$, giving

$$R_{d1}(x) = \int_x^\infty dz_1 p_1(z_1) + \int_0^x dz_1 p_1(z_1) R_{u1}(x - z_1). \qquad (6)$$

Taking Laplace transforms of both equations and solving we have

$$\widehat{R_{u1}} = \frac{\hat{p}_2 (1 - \hat{p}_1)}{s(1 - \hat{p}_1 \hat{p}_2)}, \qquad (7)$$

$$\widehat{R_{d1}} = \frac{(1 - \hat{p}_1)}{s(1 - \hat{p}_1 \hat{p}_2)}, \qquad (8)$$

where $\hat{f} = \hat{f}(s) = \int_0^\infty e^{-sx} f(x) dx$ denotes the usual Laplace transform.

Next we need the probability $Q_1(y) \delta y$ that an arbitrary point will fall in phase 1 a distance $[y, y + \delta y]$ from the left of the first down crossing on its right. The chance that the point falls on a 1-chord of length $[z_1, z_1 + dz_1]$ is

$\frac{1}{2} n_c p_1(z_1) z_1 dz_1$. The point will be uniformly distributed along the chord, therefore if it falls on a chord of length z_1 the probability that it lies a distance $[y, y + \delta y]$ from the left end is just $\delta y / z_1$. To obtain the total probability we must sum over all chords with $z > y$, giving

$$Q_1(y) \delta y = \frac{n_c}{2} \int_y^\infty dz_1 p_1(z_1) z_1 \frac{\delta y}{z_1}, \qquad (9)$$

$$\hat{Q}_1 = \frac{n_c}{2s}(1 - \hat{p}_1). \qquad (10)$$

Note that $Q_1(0) = \frac{1}{2} n_c$, as it should, since the probability that a point lies within a distance δy (to the left) of a down crossing must be $\frac{1}{2} n_c \delta y$.

Recall that $S_{11}(x)$ is the probability that two points a distance x apart fall in phase 1. The chance that the second point falls in phase 1 (given that the first does) depends on whether the distance to the first up crossing y is greater or less than the distance x. If $y > x$ then the right-hand point falls in phase 1 with unit probability. If $y < x$ then the right-hand point falls in phase 1 with probability $R_{u1}(x - y)$. Thus we have

$$S_{11}(x) = \int_x^\infty dy Q_1(y) + \int_0^x dy Q_1(y) R_{u1}(x - y). \qquad (11)$$

Note that $S_{11}(0) = \phi_1$ as it should since $S_{11}(0)$ is just the probability that a single point falls in phase 1. Taking Laplace transforms we obtain

$$\hat{S}_{11} = \frac{\phi_1}{s} - \frac{n_c}{2s^2} \frac{(1 - \hat{p}_1)(1 - \hat{p}_2)}{1 - \hat{p}_1 \hat{p}_2}. \qquad (12)$$

Two other correlation functions of the independent interval process are important for later discussions. The first, $S_{c1}(x) = \langle |I'(\mathbf{x}_1)| I(\mathbf{x}_2) \rangle$, is the 1D analog of the surface-void correlation function which arises in the study of 3D porous materials [1]. The second is the crossing-crossing correlation function $S_{cc}(x) = \langle |I'(\mathbf{x}_1)| |I'(\mathbf{x}_2)| \rangle$ analogous to the surface-surface correlation function [1]. Again, stationarity implies that S_{c1} and S_{cc} depend only on the distance $x = |\mathbf{x}_2 - \mathbf{x}_1|$.

From the definition of S_{c1} we have

$$\epsilon S_{c1}(x) \approx \left\langle \left| I\left(\mathbf{x}_1 + \frac{\epsilon}{2}\right) - I\left(\mathbf{x}_1 - \frac{\epsilon}{2}\right) \right| I(\mathbf{x}_2) \right\rangle, \qquad (13)$$

where ϵ is small. The expression on the right-hand side is the probability that x_1 lies within a distance $\epsilon/2$ (which we call an ϵ interval) of a crossing and that x_2 lies in phase 1. Without loss of generality, we consider the case $x_2 > x_1$. Now there is an equal chance of the first point landing in an ϵ interval of an up or down crossing (probability $\frac{1}{2} \epsilon n_c$). The probability that x_2 falls in phase 1 is then either $R_{u1}(x)$ or $R_{d1}(x)$. Hence, for $\epsilon \to 0$,

$$\epsilon S_{c1}(x) = \frac{1}{2} \epsilon n_c [R_{u1}(x) + R_{d1}(x)] \qquad (14)$$

or, using Laplace transforms,

$$\hat{S}_{c1} = \frac{n_c}{2s} \frac{(1-\hat{p}_1)(1+\hat{p}_2)}{1-\hat{p}_1\hat{p}_2}. \qquad (15)$$

Similarly we write the crossing-crossing correlation function as

$$\epsilon^2 S_{cc}(x) \approx \left\langle \left| I\left(\mathbf{x}_1 + \frac{1}{2}\boldsymbol{\epsilon}\right) - I\left(\mathbf{x}_1 - \frac{1}{2}\boldsymbol{\epsilon}\right) \right| \right.$$
$$\left. \times \left| I\left(\mathbf{x}_2 + \frac{1}{2}\boldsymbol{\epsilon}\right) - I\left(\mathbf{x}_2 - \frac{1}{2}\boldsymbol{\epsilon}\right) \right| \right\rangle, \qquad (16)$$

where the expression on the right is clearly the probability that both points lie within an ϵ interval of a crossing. To express this quantity in terms of the chord distributions several additional functions are needed. Let $R_{ud}(x)$ be the probability that a point a distance x from an up crossing falls in an ϵ interval of a down crossing. This can occur in two ways; either the first chord of phase 2 adjacent to the up crossing has length $z_2 = x$, or $z_2 < x$ in which case the point falls near a down crossing with probability $R_{dd}(x-z_2)$, where $R_{dd}(y)$ is the probability that a point at distance y to the right of a down crossing is in an ϵ interval of a down crossing. This is expressed as

$$R_{ud}(x) = \epsilon p_2(x) + \int_0^x dz_2 p_2(z_2) R_{dd}(x-z_2). \qquad (17)$$

The functions R_{uu}, R_{du} are similarly defined and three additional relations among the four functions can be derived and solved to give

$$\hat{R}_{ud} = \epsilon \hat{p}_2 / (1 - \hat{p}_1 \hat{p}_2), \qquad (18)$$

$$\hat{R}_{du} = \epsilon \hat{p}_1 / (1 - \hat{p}_1 \hat{p}_2), \qquad (19)$$

$$\hat{R}_{dd} = \hat{R}_{uu} = \epsilon \hat{p}_1 \hat{p}_2 / (1 - \hat{p}_1 \hat{p}_2). \qquad (20)$$

Now from the definition of S_{cc} it is clear that

$$\epsilon^2 S_{cc}(x) = \frac{1}{2} \epsilon n_c [R_{uu} + R_{ud} + R_{du} + R_{dd}] \qquad (21)$$

as $\epsilon \to 0$. After taking Laplace transforms this gives

$$\hat{S}_{cc} = \frac{n_c}{2} \frac{\hat{p}_1 + \hat{p}_2 + 2\hat{p}_1\hat{p}_2}{1 - \hat{p}_1\hat{p}_2}. \qquad (22)$$

A final expression which is useful for relating this work to prior approaches is

$$R_{1u}(x) = \epsilon f_1(x) + \int_0^x dy R_{uu}(x-y) f_1(y), \qquad (23)$$

where $R_{1u}(x)$ is the probability that a point at distance x from a point in phase 1 falls within an ϵ interval of an up crossing, and $f_1(x)$ is the probability distribution of "failure times" discussed earlier.

Although this analysis of the independent interval process, and the results for S_{c1} and S_{cc}, appear new, variants of Eq. (12) for S_{11} have actually been derived in several quite

different contexts. It is useful to briefly demonstrate these connections. The Poisson-Boolean model [2] of random two-phase media has been widely studied and applied. In this model, grains (which may be of different shapes and sizes) are placed at uncorrelated random points in space (so the grains may overlap). For spherical inclusions this is just the overlapping sphere (or Swiss-cheese) model [1]. For convex grains of any shape or size, the chord-distribution function of the phase exterior to the grains is $p_1(z) = \lambda \exp(-\lambda z)$ where $\lambda = s_v / 4\phi_1$. Since the grains are uncorrelated in space and convex it is clear that the length of successive chords along any line through a realization of the model will be independent. Therefore Eq. (12) applies. Specializing to Boolean models [$\hat{p}_1 = \lambda / (\lambda + s)$] we recover the well known result (e.g., Ref. [4])

$$\frac{s\hat{S}_{11}}{\phi_1} = \frac{1-\hat{p}_1}{1-\hat{p}_1\hat{p}_2}. \qquad (24)$$

Since $S_{11}(x)$ is known for many Boolean models, this result allows p_2 to be calculated:

$$\hat{p}_2 = 1 + s/\lambda - \phi_1/\lambda\hat{S}_{11}. \qquad (25)$$

Let us further specialize to the case of a 1D Boolean process where the grains are rods with random lengths distributed according to the cumulative distribution function $\Psi(z)$. For this model $S_{11}(x) = \phi_1 \exp\{-\lambda\int_0^x[1-\Psi(z)]dz\}$ and the formula for $\hat{p}_2$ becomes a well known result for the busy period in an $M/G/\infty$ queue [20,30].

The independent interval process is useful in the interpretation of small-angle x-ray scattering data. In Refs. [5,26] the Fourier transform of $d^2 S_{11}/dx^2$ was derived in terms of the Fourier transforms of the chord functions. The result can be shown to be equivalent to Eq. (12). Rice's [23] formulas for S_{11} for two different types of random telegraph signal can also be rederived using Eq. (12). In the next section we show how the independent interval process can be used to derive useful approximations of the chord functions for the single level-cut Gaussian random field (GRF) model.

IV. CHORD FUNCTIONS OF LEVEL-CUT GAUSSIAN RANDOM FIELDS

A Gaussian field is statistically specified in terms of a field-field correlation function $\langle y(r_1) y(r_2) \rangle = g(|\mathbf{r}_2 - \mathbf{r}_1|)$ [23,31]. Here we consider isotropic stationary fields with zero mean [$\langle y(\mathbf{r}) \rangle = 0$] and unit variance [$\langle y^2(\mathbf{r}) \rangle = g(0) = 1$]. Many methods exist for generating GRF's with a given $g(r)$. For example, in 1D we have

$$y(x) = \sum_{i=1}^N a_i \cos k_i x + b_i \sin k_i x, \quad k_i = \frac{2\pi i}{T}, \qquad (26)$$

where a_i and b_i are independent Gaussian random variables with mean zero and $\langle a_i^2 \rangle = \langle b_i^2 \rangle = (2\pi/T)F(k_i)$. In the limit $N, T \to \infty$ such that $N/T \to \infty$ the correlation function is $g(x) = \int_0^\infty F(k)\cos(kx)dk$. $F(k)$ is called a spectral density. When $F(k)$ is a wide or narrow distribution, the process is, respectively, said to be wide or narrow band. The 3D analog is

$$y(\mathbf{r}) = \sum_{l=-N}^{N} \sum_{m=-N}^{N} \sum_{n=-N}^{N} c_{lmn} e^{i\mathbf{k}_{lmn}\cdot\mathbf{r}}, \qquad (27)$$

where $\mathbf{k}_{lmn} = (2\pi/T)(l\mathbf{i} + m\mathbf{j} + n\mathbf{k})$ and $c_{l,m,n} = a_{lmn} + ib_{lmn}$. For y real and $\langle y \rangle = 0$ we take $c_{l,m,n} = \bar{c}_{-l,-m,-n}$ and $c_{0,0,0} = 0$. As above, a_{lmn} and b_{lmn} have mean zero and $\langle a_{lmn}^2 \rangle = \langle b_{lmn}^2 \rangle = \frac{1}{2}(2\pi/T)^3 \rho(k_{lmn})$. In this case $g(r) = 4\pi r^{-1} \int_0^\infty 4\pi k \rho(k) \sin kr \, dk$. A two-dimensional random field is shown in Fig. 1(a).

A two-phase level-cut GRF model is specified by the microstructure indicator function $I(\mathbf{r}) = H(\beta - y(\mathbf{r}))$, where H is the Heaviside step function. There are two very useful properties of the Gaussian model. First the random field is ergodic (ensemble averages equal spatial averages), and second the variables $y(\mathbf{r}_i)$ $i = 1,2,3\ldots$ and their spatial derivatives $[\nabla y(\mathbf{r}_i)$, etc.] are correlated Gaussian random variables with known joint probability distribution. This allows many useful statistical properties of the thresholded model (such as S_{11}) to be calculated.

In the preceding section we derived the properties of the independent interval process in terms of p_1 and p_2. However, it is clear that if any two of the microstructure functions (p_1, p_2, S_{11}, S_{c1}, S_{cc}) are known the remainder can be determined by means of Eqs. (12), (15), and (22). Since S_{11}, S_{c1}, and S_{cc} can be calculated for the level-cut GRF model, this allows an approximation to be derived for the chord functions. The accuracy of the results will then depend on the validity of the hypothesis that successive chords of the model are uncorrelated (or nearly so). For simplicity we consider the case where S_{11} and S_{c1} are known. Simultaneous solutions of Eqs. (12) and (15) then give

$$\hat{p}_1 = \frac{n_c - s(\hat{S}_{c1} - s\hat{S}_{11} + \phi_1)}{n_c - s(\hat{S}_{c1} + s\hat{S}_{11} - \phi_1)}, \qquad (28)$$

$$\hat{p}_2 = \frac{\hat{S}_{c1} + s\hat{S}_{11} - \phi_1}{\hat{S}_{c1} - s\hat{S}_{11} + \phi_1}. \qquad (29)$$

This result can be considered a generalization of a recent approximation developed independently by the authors of Refs. [27] and [28]. In a study of the zero-threshold case [where $p(z) = p_1(z) = p_2(z)$] they found

$$\hat{p} = \frac{n_c + s(2\hat{S}_{11} - 1)}{n_c - s(2\hat{S}_{11} - 1)}, \qquad (30)$$

where $S_{11}(x) = \frac{1}{4} + (1/2\pi)\arcsin[g(x)]$. This result is obtained by substituting $\phi_1 = \phi_2 = \frac{1}{2}$ and $S_{c1} = n_c/2$ (which is true for any symmetric medium) into Eqs. (28) and (29). The result provided an excellent approximation for the case $g(x) = [1/\cosh(x/2)]^{d/2}$ $(d = 1,2,3)$.

Clearly other approximations can be obtained using the independent interval process, and several have been previously given. For example, Eq. (17) was obtained by McFadden [25] and Rice [32], and approximate forms of Eq. (23) have been used to obtain the distribution of failure times [22]. If the chords are uncorrelated all the methods will give identical results. An advantage of approximation (30) and its generalization [Eqs. (28) and (29)] is that S_{11} and S_{c1} are

relatively simple to evaluate; the functions R_{uu}, R_{dd}, and R_{ud} appearing in the integral equations Eqs. (17) and (23) are quite complex for a nonzero threshold [32].

To evaluate the approximations for an arbitrary threshold we have the following results:

$$\phi_1 = \frac{1}{2} + \frac{1}{2}\mathrm{erf}\frac{\beta}{\sqrt{2}}, \quad n_c = \frac{\gamma}{\pi}e^{-(1/2)\beta^2}, \qquad (31)$$

$$S_{11} = \phi_1^2 + \frac{1}{2\pi}\int_0^{g(x)} \frac{dt}{\sqrt{1-t^2}}\exp\left(-\frac{\beta^2}{1+t}\right), \qquad (32)$$

$$S_{c1} = \frac{n_c}{2} + \frac{n_c}{2}\mathrm{erf}\left[\frac{\gamma\beta(1-g)}{\sqrt{2|G|}}\right]$$
$$- \frac{g'\exp[-\beta^2/(1+g)]}{2\pi\sqrt{1-g^2}}\mathrm{erf}\left[\frac{\beta}{\sqrt{2|G|}}g'\sqrt{\frac{1-g}{1+g}}\right], \qquad (33)$$

where $\gamma = \sqrt{-g''(0)}$ and $|G| = \gamma^2[1 - g^2(x)] - [g'(x)]^2$. The results for n_c [23] and S_{11} [13] are well known, and the final expression for S_{c1} can be evaluated using the method of Rice as follows. For the level-cut Gaussian random field, we have

$$S_{c1} = \langle \delta(\beta - y(x_1)) | y'(x_1) | H(\beta - y(x_2)) \rangle. \qquad (34)$$

The variables $\mathbf{w} = [w_1, w_2, w_3] = [y(x_1), y(x_2), y'(x_1)]$ have Gaussian distributions with cross correlation matrix

$$g_{ij} = \langle w_i w_j \rangle \Rightarrow G = \begin{bmatrix} 1 & g(x) & 0 \\ g(x) & 1 & -g'(x) \\ 0 & -g'(x) & -g''(0) \end{bmatrix} \quad (35)$$

for $x = |x_2 - x_1|$ and $x_2 > x_1$. If $x_2 < x_1$, $\langle y(x_1)y'(x_2) \rangle = g'(|x|)$ but this does not affect the final result. To find S_{c1} we must therefore evaluate

$$\int\int\int d\mathbf{w}\, \delta(\beta - w_1) H(\beta - w_2) |w_3| \frac{e^{-(1/2)\mathbf{w}^T G^{-1}\mathbf{w}}}{(2\pi)^{3/2}|G|^{1/2}}. \qquad (36)$$

The integrals extend over all space and the final factor is just the joint probability density function of w_i. The result is given in Eq. (33).

To obtain p_i it is necessary to invert Eqs. (28) and (29). This can be done using a short and efficient algorithm [33]. As previously noted, $\hat{p}_i$ needs to be known to around nine significant figures to achieve four significant figure accuracy in the result [30]. To minimize cancellation errors in the numerators and save one integration, we rewrite Eqs. (28) and (29) as

$$\hat{p}_1 = \frac{\widehat{S''_{11}} - s\widehat{S^T_{c1}}}{n_c - \widehat{S''_{11}} - s\widehat{S^T_{c1}}}, \qquad (37)$$

$$\hat{p}_2 = \frac{\widehat{S_{11}''} + s\widehat{S_{c1}^T}}{n_c - \widehat{S_{11}''} + s\widehat{S_{c1}^T}}, \tag{38}$$

where $S_{c1}^T(x) = S_{c1}(x) - \frac{1}{2}n_c$. The Laplace transforms $\widehat{S_{11}''}(s)$ and $\widehat{S_{c1}^T}(s)$ on the right-hand side of Eqs. (37) and (38) can be evaluated using numerical quadrature.

To check the validity of the independent interval approximation, we measure the chord distribution directly from realizations of the thresholded model. This is simpler (and minimizes finite-size effects) in one dimension. A 1D random process $y_1(x)$ can be obtained from a 3D GRF $y_3(\mathbf{r})$ by taking $y_1(x) = y_3(\mathbf{r}_0 + \hat{\mathbf{n}}x)$ where $\mathbf{r}_0$ is an arbitrary origin and $\hat{\mathbf{n}}$ is a unit vector with arbitrary orientation. Now $y_1(x)$ can be generated independently of $y_3(\mathbf{r})$ by using the 1D definition for $y(x)$ given in Eq. (26). To ensure that $y(x)$ and $y_1(x)$ are statistically identical they must share $g(x)$. This is true if $F(k) = 4\pi\int_k^\infty s\rho(s)ds$, where F and ρ are, respectively, the spectral densities of the 1D and 3D random fields. This shows that $F(k)$ must be a nondecreasing function for 1D random processes obtained from 3D random fields.

In the modeling of random media, the following Fourier transform pairs $[g(x)$ and $\rho(k) = -F'(k)/(4\pi k)]$ have proved useful:

$$g_a = e^{-x/\xi}\left(1 + \frac{x}{\xi}\right), \tag{39}$$

$$F_a = \frac{4\xi}{\pi(1 + \xi^2 k^2)^2}, \tag{40}$$

$$g_b = e^{-x^2/l_0^2}, \tag{41}$$

$$F_b = \frac{l_0}{\sqrt{\pi}}e^{-(1/4)k^2 l_0^2}, \tag{42}$$

$$g_c = e^{-x/\xi}(1 + x/\xi)\frac{\sin 2\pi x/d}{2\pi x/d}, \tag{43}$$

$$F_c = \frac{d}{2\pi^2}\left(\tan^{-1}c_- + \tan^{-1}c_+ + \frac{c_+}{1 + c_+^2} + \frac{c_-}{1 + c_-^2}\right),$$

$$c_\pm = z\left(\frac{2\pi}{d} \pm k\right). \tag{44}$$

For a finite number of crossings per unit length (or specific surface in three dimensions) it is necessary that $g'(0) = 0$ [23]. For simplicity we restrict attention to the following parameters which give $\gamma = \sqrt{-g''(0)} = 1$ μm^{-1}: (a) $\xi = 1$ μm; (b) $l_0 = \sqrt{2}$ μm; and (c) $\xi = \sqrt{2}$ μm, $d = 4\pi/\sqrt{6}$ μm. A cross section of the two-phase medium generated in each of the three cases is shown in Figs. 2(a)–2(c). We have checked the approximation in the volume fraction range $\phi_1 \in [0.1, 0.9]$; results for $\phi_1 = 0.2$ are shown in Fig. 2 (and are typical of those at other volume fractions). The independent interval approximation is seen to provide remarkably accurate estimates of the measured chord distributions.
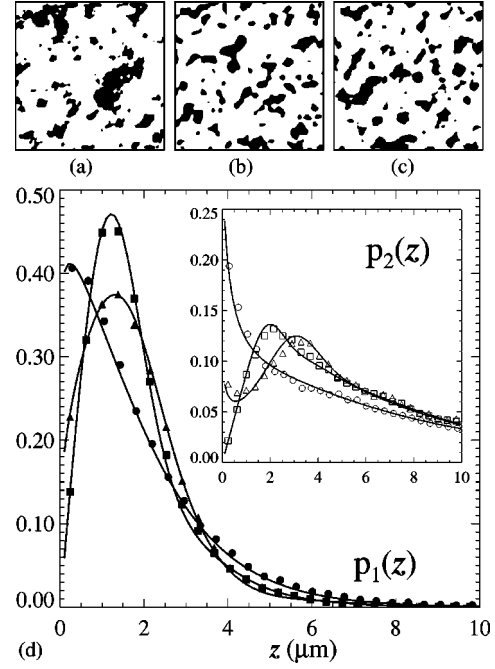

FIG. 2. Chord functions of single-cut Gaussian random fields at volume fraction $\phi_1 = 0.2$. The symbols are directly measured from simulations, and the lines correspond to the independent interval approximation. The models [see Eqs. (39)–(44)] are shown in the top row with side length 40 μm: (a) $g_a(x)$, $\bigcirc$; (b) $g_b(x)$, $\square$; (c) $g_c(x)$, $\triangle$. The chord functions correspond to the first-passage time problem considered by Rice.

The largest deviations between simulation and the approximation are seen for the oscillatory correlation function $g_c(x)$. We can investigate this ''narrow-band'' limit by taking $\xi \to \infty$ in $g_c(x)$, which gives

$$g_d(x) = \frac{\sin 2\pi x/d}{2\pi x/d}, \tag{45}$$

$$F_d = \frac{d}{2\pi}H\left(\frac{2\pi}{d} - k\right). \tag{46}$$

The results for p_1 at volume fractions $\phi_1 = 0.2, 0.5$, and 0.8 are shown in Fig. 3, and $S_{11}(x)$ is in Fig. 4. At $\phi_1 = 0.5$ the approximation is equivalent to that of Refs. [27,28]. The approximation breaks down after one wavelength d and actually falls below zero (which is not inconsistent with the derivation). This is because the process [see Fig. 3(a)] has approximately periodic regions, extending over several wavelengths, which implies some level of correlation between adjacent chords. For example, at $\phi_1 = 0.5$, a chord of length $\approx \frac{1}{2}d$ is more likely to be followed by another of approximately the same length than if it were randomly chosen according to the probability distribution $p_2(z)$. This contradicts the assumptions of the independent interval approximation. The oscillations in the autocorrelation function (Fig. 4) clearly reflect appreciable order in the system.

Note that $g_d(x)$ represents the worst-case (or most narrow-band) process corresponding to a 3D field since $\rho_d(k) \propto \delta(2\pi/d - k)$ (i.e., an infinitely narrow band pass filter). However, the related 1D process corresponds to a low pass filter (i.e., it is not strongly narrow band). This shows
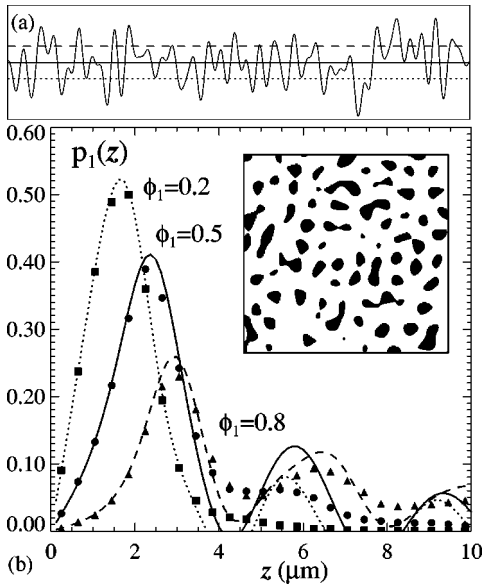
FIG. 3. The phase 1 chord function of a level-cut GRF with $g(x)=\sin(kx)/(kx)$ ($k=\sqrt{3}$ μm) at three different volume fractions. The inset shows the microstructure at $\phi_1=0.2$ (side length 40 μm). A 1D transect (length 150 μm) of the random field is shown in (a). The horizontal lines correspond to the threshold at each volume fraction. The independent interval assumption breaks down because the process is nearly periodic in some regions.

that approximations valid for medium- and wide-band Gaussian random processes are sufficient to reproduce the chord functions of 3D models based on random fields. The failure of the independent interval approximation in this narrow-band limit is not critical for two reasons. First, the model $g_c(x)$ (with $\xi>0$, for which the approximation is reasonable) has been found more relevant to physical materials than model $g_d(x)$ (e.g., see Sec. VI). Second, even in the worst case, the approximation remains useful out to one wavelength. This may prove adequate for material characterization.

V. EXTENSION TO MORE COMPLEX MODELS

So far our results have been concerned with the conventional first-time distributions associated with an arbitrary threshold (β) of a Gaussian random process. However, the
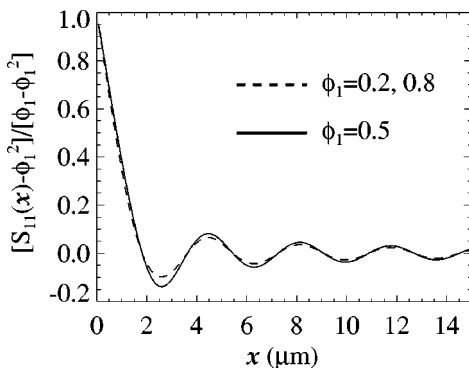

FIG. 4. The normalized two-point correlation function [Eq. (32)] of the random model shown in Fig. 3. The strong oscillations in $S_{11}(x)$ correspond to periodic correlations in the microstructure.
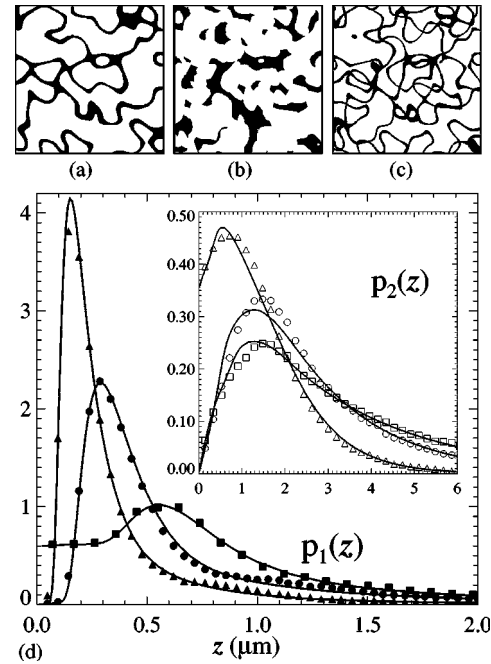

FIG. 5. The independent interval approximation compared with simulations of the chord functions for three distinct models based on level-cut Gaussian random fields: (a) Berk's two-cut model, $\bigcirc$; (b) the intersection set of two two-cut models, $\square$; (c) the union set of two two-cut models, $\triangle$. The side length of the images is 15 μm.

single-cut random field model is not sufficiently general to model the microstructure of many interesting materials. To model the bicontinuous structure of microemulsions, Berk [13] suggested that phase 1 be defined as the region in space where $\alpha<y(\mathbf{r})<\beta$, this is the so-called two-cut model [Fig. 5(a)]. The two-cut model has also proven useful in interpreting conductivity and percolation behavior in polymer blends [34]. Open cell foams (e.g., aerogels) and the porous network of sandstones have been modeled by the intersection sets of two statistically identical (but independent) two-cut fields [Fig. 5(b)], and closed cell foams may be modeled by the union of two such structures [Fig. 5(c)] [8]. Our method can be simply extended to these problems.

For Berk's [13] two-cut model, we have

$$\phi_1=\frac{1}{2}\mathrm{erf}\frac{\beta}{\sqrt{2}}-\frac{1}{2}\mathrm{erf}\frac{\alpha}{\sqrt{2}},\qquad(47)$$

$$n_c=\frac{\sqrt{\gamma}}{\pi}(e^{-(1/2)\beta^2}+e^{-(1/2)\alpha^2}),\qquad(48)$$

$$S_{11}=\phi_1^2+\frac{1}{2\pi}\int_0^{g(x)}\frac{dt}{\sqrt{1-t^2}}\times\left[\exp\left(\frac{-\alpha^2}{1+t}\right)\right.$$
$$\left.-2\exp\left(\frac{2\alpha\beta t-\alpha^2-\beta^2}{2(1-t^2)}\right)+\exp\left(\frac{-\beta^2}{1+t}\right)\right],\quad(49)$$

$$S_{c1}=f_{\beta\beta}+f_{\beta\alpha}-f_{\alpha\beta}-f_{\alpha\alpha},\qquad(50)$$

where

$$f_{\alpha\beta} = \langle H(\alpha - y(x_1))\delta(\beta - y(x_2))|y'(x_2)|\rangle$$

$$= \frac{\sqrt{\gamma}e^{-(1/2)\beta^2}}{2\pi}\left(1 + \mathrm{erf}\left[\sqrt{\frac{\gamma}{2|G|}}(\alpha - \beta g)\right]\right) \quad (51)$$

$$- \frac{g'}{2\pi\sqrt{1-g^2}}\exp\left(-\frac{1}{2}\frac{\alpha^2 - 2\alpha\beta g + \beta^2}{1-g^2}\right)$$

$$\times \mathrm{erf}\left[\frac{\alpha - \beta g}{\sqrt{2|G|}}\frac{g'}{\sqrt{1-g^2}}\right]. \quad (52)$$

Using these results we can directly apply the approximation for the chord distributions. We use the field-field function $g_b(x)$ with $l_0 = \sqrt{2}$ μm and consider a ''centered'' two-cut field ($\alpha = -\beta$) at volume fraction $\phi = 0.2$. The results are shown as circles in Fig. 5 and show very good agreement with simulations.

To evaluate the chord functions of the intersection and union sets we first derive their statistical properties. Suppose $\Omega(\mathbf{x})$ and $\Psi(\mathbf{x})$ are the indicator functions of two independent, but statistically identical, models of random media with properties ϕ_1, n_c, S_{11}, and S_{c1}. A new model is obtained by forming the intersection set of Ω and Ψ which has indicator function $I(\mathbf{x}) = \Omega(\mathbf{x}) \times \Psi(\mathbf{x})$. Clearly $\phi_1^I = \langle I \rangle = \langle \Omega \rangle \langle \Psi \rangle = \phi_1^2$ and $n_c^I = \langle |I'| \rangle = \langle |\Omega'\Psi + \Omega\Psi'| \rangle = \langle |\Omega'|\Psi + \Omega|\Psi'| \rangle = 2\langle\Omega\rangle\langle|\Omega'|\rangle = 2\phi_1 n_c$. The relation $|\Omega'\Psi + \Omega\Psi'| = |\Omega'|\Psi + \Omega|\Psi'|$ is true everywhere except where the interface of Ψ and Ω intersects. The contribution of this error to the final result is negligible. A similar reasoning can be applied to find S_{11}^I and S_{c1}^I, as well as corresponding results for an analogously defined union set with indicator function $I(\mathbf{x}) = \Omega(\mathbf{x}) + \Psi(\mathbf{x}) - \Omega(\mathbf{x}) \times \Psi(\mathbf{x})$. In summary the results needed to apply the approximation for the chord-distribution function are

$$\phi_1^I = (\phi_1)^2, \quad (53)$$

$$n_c^I = 2\phi_1 n_c, \quad (54)$$

$$S_{11}^I = (S_{11})^2, \quad (55)$$

$$S_{c1}^I = 2S_{11}S_{c1}, \quad (56)$$

$$\phi_1^U = \phi_1(2 - \phi_1), \quad (57)$$

$$n_c^U = 2(1 - \phi_1)n_c, \quad (58)$$

$$S_{11}^U = 2(\phi_1)^2 + 2S_{11}(1 - 2\phi_1) + (S_{11})^2, \quad (59)$$

$$S_{c1}^U = 2S_{c1}(1 - 2\phi_1 + S_{11}) + 2n_c(\phi_1 - S_{11}). \quad (60)$$

Here the unsuperscripted microstructure properties correspond to the primary models Ω and Ψ and the superscripted (I or U) functions are to be used in Eqs. (28) and (29).

Although Eqs. (53)–(60) are true for any independent random models, we restrict attention to the case where the primary sets are obtained from Berk's model [see Eqs. (47)–(50) and Fig. 5(a)]. As above we consider centered models ($\alpha = -\beta$) at volume fraction $\phi_1 = 0.2$ obtained from random fields with correlation function $g_b(x)$ ($l_0 = \sqrt{2}$ μm). The
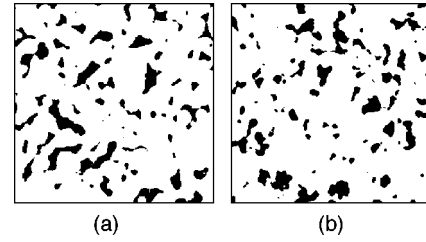

(a)   (b)

FIG. 6. A binarized image of a silver-tungsten composite [35] (a) compared with a model [36] based on a level-cut Gaussian random field (b). The side length is 99.4 μm. The parameters and the model are chosen to reproduce the experimental two-point function and chord-distribution function (see Fig. 7).

results of the independent interval approximation are compared with simulations in Fig. 5. In general the approximation is excellent. For $r < 3$ μm significant deviations (up to 10%) are seen between the calculated and simulated values of the chord distribution of phase 2 (p_2).

VI. APPLICATION TO POROUS AND COMPOSITE MATERIALS

To study the properties of a random medium it is important to have an accurate model of the microstructure. If the physical mechanisms responsible for the evolution of the microstructure are not well known (or difficult to simulate) an empirically based statistical model may be useful [8–10,12,16]. The level-cut GRF model is well suited to this approach because of its generality: the morphology of the model may be ''tuned'' to some degree to match that of the random medium. The simplest and most common morphological quantities are the density (or porosity) and the two-point correlation function, which can both be measured from a cross-sectional image. It is possible to generate a GRF model with approximately the same statistical properties by an appropriate choice of parameters [8,12,16].

As an example we show a binarized image of a tungsten-silver composite [35] along side a single-cut GRF model in Fig. 6. The parameters of the model were derived in Ref. [36] as follows. The level-cut parameter is taken as $\beta = -0.84$ so that the silver volume fraction $\phi_1 = 0.2$ is exactly that of the composite [Eq. (31)]. The random field is generated using $\rho_c(k)$ [Eq. (44)]. The length scales of the random field $\xi = 2.15$ μm and $d = 13.0$ μm are chosen (by a nonlinear least squares method) so that the two-point correlation function of the model matches that of the composite. The theoretical and experimental values of $S_{11}(r)$ (which are practically indistinguishable) are shown in the inset of Fig 7. Since the volume fraction and two-point function do not uniquely specify a random microstructure (i.e., many different models may reproduce these morphological quantities [8]), it is necessary to test the results. The chord functions are ideal in this regard as they provide a strong signature of microstructure and can be measured from a cross-sectional image. The independent interval approximation and experimental data are compared in Fig. 7. The reasonable agreement between theory and experiment indicates that the model is capturing important features of the tungsten-silver composite.
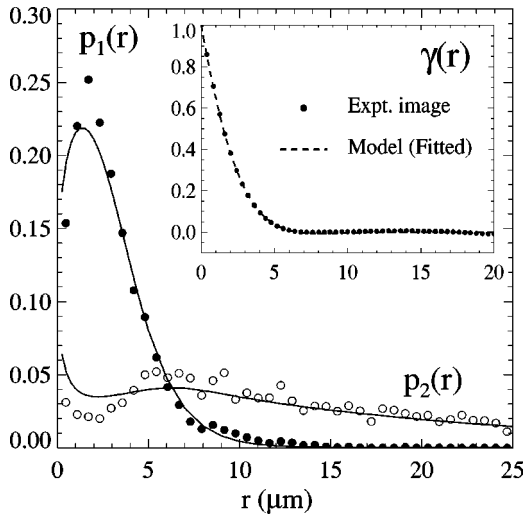
FIG. 7. The main graph shows a comparison between the chord functions of a silver-tungsten composite (symbols) and the results of the independent interval approximation for a level-cut Gaussian random field model. The composite and model are shown in Fig. 6. The inset compares the experimental and model autocorrelation function $\gamma(x) = [S_{11}(x) - \phi_1^2]/(\phi_1 - \phi_1^2)$.

A second example is provided by a digitized image of Fontainebleau sandstone obtained by x-ray tomography [37,38]. To mimic the granular character of the sandstone [Fig. 8(a)] we use a model based on the intersection set of $n(=5)$ single-cut Gaussian random fields. The result is shown in Fig. 8(b). To match the porosity of the model with that of the sandstone ($\phi = 0.154$), we take $\beta = 0.48$ for each of the five primary random field models. This corresponds to $\phi_1 = (0.154)^{1/5}$. The experimental two-point function is reproduced by choosing $\xi = 51.9 \ \mu$m and $d = 272 \ \mu$m in model $g_c(r)$ (by a least squares method). The independent interval approximation for the chord functions is calculated using the relations $S_{11}^I = (S_{11})^n$ and $S_{c1}^I = n(S_{11})^{n-1}S_{c1}$ [which are a straightforward extension of Eqs. (55) and (56)]. The results are shown in Fig. 9. The model is able to mimic the two-point function extremely well, and the chord functions with good accuracy. This provides evidence that the model is reasonable. 3D images of the model and sandstone microstructures are shown in Figs. 10 and 11. The sandstone appears more well connected than the model, the model showing more isolated pores. This is actually an artifact of the method used to plot the pore-solid interface. An
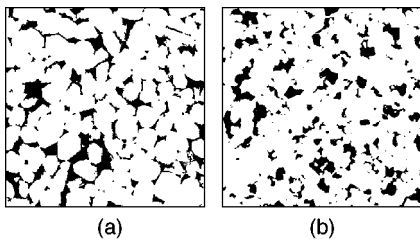

FIG. 8. A cross section of Fontainebleau sandstone (a) compared with a model [36] based on the intersection set of five level-cut Gaussian random fields (b). The side length is 2.18 mm. The statistical properties of the sandstone and model are compared in Fig. 9.
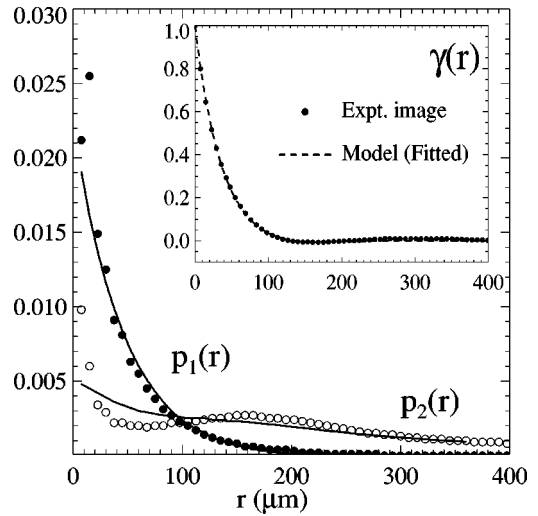

FIG. 9. The chord functions measured from a 3D image of Fontainebleau sandstone (symbols) compare well with the results of the independent interval approximation (main graph) for a Gaussian random field model. The inset shows the autocorrelation function $\gamma(x) = [S_{11}(x) - \phi_1^2]/(\phi_1 - \phi_1^2)$. Three-dimensional realizations of the sandstone and the model are shown in Figs. 10 and 11, respectively.

algorithm was used to determine that 98.8% of the pore space in the model is connected to the outer faces, which compares well with 99.6% for the sandstone. Therefore the model is also able to capture the interconnections of the sandstone pores.

VII. CONCLUSION

We have derived a semianalytic approximation for the chord-distribution functions (p_1 and p_2) of 3D random media. The approximation is based on the assumption that successive chord lengths are uncorrelated. The result can be applied to models for which the two-point (S_{11}) and 1D ''surface-void'' (S_{c1}) correlation functions can be evaluated. The calculation of S_{11} and S_{c1} is generally much easier than calculation of p_1 and p_2. The result is exact for Boolean
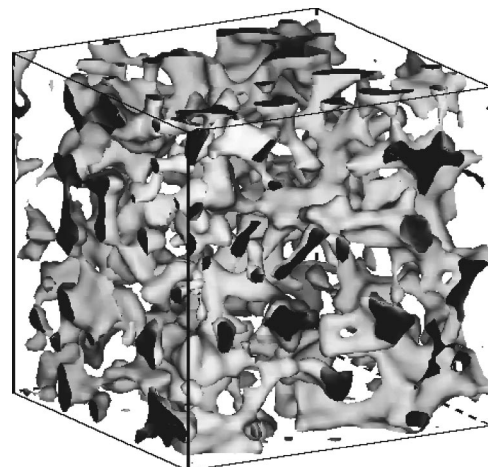

FIG. 10. 3D representation of Fontainebleau sandstone sample obtained by x-ray tomography [37,38]. The pore space is shown as solid to aid visualization. The side length of the image is 960 μm.
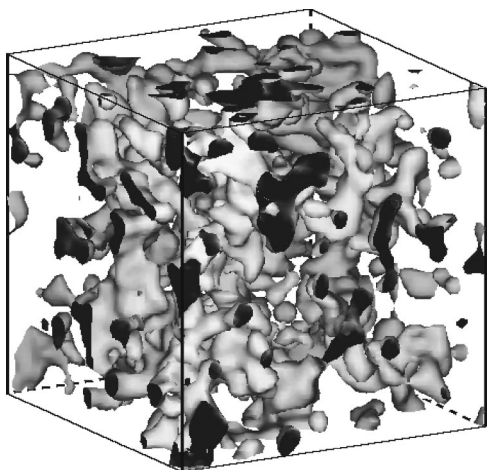
FIG. 11. A sandstone model based on Gaussian random fields (cf. Fig. 10). The independent interval approximation for the chord distribution shows reasonable agreement with experimental data (Fig. 9). Many of the apparently isolated regions of pore space (shown as solid) are artifacts of the plotting procedure.

models with convex grains since the assumption of independent intervals is true. We have applied the approximation to the single level-cut Gaussian random field model of random materials. In this case the chord functions correspond to Rice's first-passage time distribution for random noise. The approximation is very accurate for wide-band random fields, but loses accuracy after one ''wavelength'' of the field for extremely narrow-band (approximately periodic) fields. Note that a narrow-band field corresponds to a low pass (rather than a narrow pass) filtered process in 1D.

The result also gives accurate results for Berk's two-cut GRF model and other models based on the intersection and union sets of level-cut GRF's. This is important for generating 3D models of random media using empirical information

measured from cross-sectional images; the two-point correlation function does not necessarily provide sufficient information, and good approximations for the chord functions are very useful. In this context it is possible to apply the approximation confidently if the two-point correlation function exhibits no (or weak) oscillations. To demonstrate the application of our results we have compared the approximation to experimental data obtained from images of a tungsten-silver composite and a porous sandstone.

In order to derive the chord function approximation we studied the independent interval process in detail. We have shown that the process underlies the derivation, and provides useful links between, important results in many different fields. The general treatment of the process makes clear the relation between various approximations for different first-passage times made in signal theory, the analysis of component failure and persistence times in coarsening. From the expressions for $\hat{p}_i$ [Eqs. (28) and (29)] it is simple to obtain the lineal-path functions as $L_i = \mathcal{L}^{-1}\{\phi_i/s - n_c[1 + \hat{p}_i(s)]/2s^2\}$. For $i=1$ this is just the ''survival probability'' in the context of random processes. Similarly the probability density of ''time to failure'' given that $t=0$ falls in a safe region is $f_1 = \mathcal{L}^{-1}\{n_c[1 - \hat{p}_1(s)]/2\phi_1 s\}$. These expressions can be inverted in the same way as p_i. Due to its apparent generality it would be useful to explore the properties of the process further. Extensions to include correlation between the chord lengths and the development of a 3D analog would be useful future studies.

ACKNOWLEDGMENTS

[1] S. Torquato, Appl. Mech. Rev. **44**, 37 (1991).

[2] J. Serra, *Image Analysis and Mathematical Morphology* (Academic Press, London, 1988).

[3] E. E. Underwood, *Quantitative Stereology* (Addison-Wesley, Reading, MA, 1970).

[4] R. P. King, Chem. Eng. J. **52**, 1151 (1996).

[5] P. Levitz and D. Tchoubar, J. Phys. I **2**, 771 (1992).

[6] T. K. Tokunaga, J. Chem. Phys. **82**, 5298 (1985).

[7] S. Torquato and B. Lu, Phys. Rev. E **47**, 2950 (1993).

[8] A. P. Roberts, Phys. Rev. E **56**, 3203 (1997).

[9] F. S. Bourgeois and G. J. Lyman, Chem. Eng. Sci. **52**, 1151 (1997).

[10] C. L. Y. Yeong and S. Torquato, Phys. Rev. E **58**, 224 (1998).

[11] R. W. Hopper, J. Non-Cryst. Solids **145**, 263 (1982).

[12] J. A. Quiblier, J. Colloid Interface Sci. **98**, 84 (1984).

[13] N. F. Berk, Phys. Rev. A **44**, 5069 (1991).

[14] R. Blumenfeld and S. Torquato, Phys. Rev. E **48**, 4492 (1993).

[15] A. P. Roberts and M. Teubner, Phys. Rev. E **51**, 4141 (1995).

[16] P. M. Adler, *Porous Media* (Butterworth-Heinemann, Boston, 1992).

[17] P. Levitz, Adv. Colloid Interface Sci. **76-77**, 71 (1998).

[18] R. Zeitak, Phys. Rev. E **56**, 2560 (1997).

[19] A. J. Rainal, IEEE Trans. Inf. Theory **34**, 1383 (1988).

[20] P. Hall, *Introduction to the Theory of Coverage Processes* (Wiley, New York, 1988).

[21] K. Podgórski, I. Rychlik, and U. E. B. Machado (unpublished).

[22] S. R. K. Nielsen, J. Sound Vib. **137**, 305 (1990).

[23] S. O. Rice, Bell Syst. Tech. J. **23**, 282 (1944); **24**, 46 (1945).

[24] A. J. F. Siegert, Phys. Rev. **81**, 617 (1951).

[25] J. A. McFadden, IRE Trans. Inf. Theory **IT-2**, 146 (1956); **4**, 14 (1957).

[26] J. Méring and D. Tchoubar, J. Appl. Crystallogr. **1**, 153 (1968).

[27] B. Derrida, V. Hakim, and R. Zeitak, Phys. Rev. Lett. **77**, 2871 (1996).

[28] S. N. Majumdar, C. Sire, A. J. Bray, and S. J. Cornell, Phys. Rev. Lett. **77**, 2867 (1996).

[29] E. H. Vanmarcke, J. Appl. Mech. **42**, 215 (1975).

[30] J. Quintanilla and S. Torquato, Phys. Rev. E **54**, 4027 (1996).

[31] R. J. Adler, *The Geometry of Random Fields* (Wiley, Chichester, 1981).

[32] S. O. Rice, Bell Syst. Tech. J. **37**, 581 (1958).

[33] J. Abate and W. Whitt, ORSA J. Comput. **7**, 36 (1995).

[34] M. A. Knackstedt and A. P. Roberts, Macromolecules **29**, 1369 (1996).

[35] S. Umekawa, R. Kotfila, and O. D. Sherby, J. Mech. Phys. Solids **13**, 229 (1965).

[36] A. P. Roberts and E. J. Garboczi (unpublished).

[37] L. M. Schwartz, F. Auzerais, J. Dunsmuir, N. Martys, D. P. Bentz, and S. Torquato, Physica A **207**, 28 (1994).

[38] D. A. Coker, S. Torquato, and J. H. Dunsmuir, J. Geophys. Res. **101**, 17 497 (1996).